Published in final edited form as:
Nephron Exp Nephrol. 2009 ; 112(2): . doi:10.1159/000213505.

Microarray and bioinformatics analysis of gene expression in experimental membranous nephropathy

Peter V. Hauser[1,†,*], **Paul Perco**[3,4,5,*], **Irmgard Mühlberger**[5], **Jeffrey Pippin**[1], **Mary Blonski**[1], **Bernd Mayer**[5], **Charles E. Alpers**[2], **Rainer Oberbauer**[3,4], and **Stuart J. Shankland**[1]

[1]Division of Nephrology & Hypertension, University of Washington, Seattle, WA, USA

[2]Department of Pathology, University of Washington, Seattle, WA, USA

[3]Department of Nephrology, KH Elisabethinen, Linz, Austria

[4]Department of Nephrology, Medical University of Vienna, Austria

[5]emergentec biodevelopment GmbH

Abstract

Background—Passive Heymann Nephritis (PHN), the best characterized animal model of experimental membranous nephropathy, is characterized by subepithelial immune deposits, podocyte foot processes effacement and massive proteinuria beginning 4 days following disease induction. Although single genes involved in PHN have been studied, no whole genome wide expression analysis of kidney tissue has been performed.

Methods—Microarray analysis was performed to identify gene expression changes in PHN rat kidneys during the onset of proteinuria.

Results—Our results showed that 234 transcripts were differentially expressed in diseased animals compared to controls. Genes exclusively upregulated in diseased animals, were mainly required for cell structure and motility, immunity and defence, cell cycle, and developmental processes. The single most increased gene was transgelin (Tagln) showing a 70-fold upregulation in animals with PHN. Protein-protein interaction analysis revealed the following four processes of major relevance in disease manifestation: (i) DNA damage and repair; (ii) changes in the extra cellular matrix; (iii) deregulation of cytokines and growth factors, as well as (iv) rearrangements of the cytoskeleton.

Conclusion—We show for the first time the complex interplay between multiple different genes in experimental membranous nephropathy, supporting a role for genomic approaches to better understanding and defining specific disease processes.

Keywords

passive Heymann nephritis (PHN); gene expression profiling; human nephritis; proteinuria; microarray; bioinformatics; podocyte

Correspondence: Peter V. Hauser, PhD, Division of Nephrology, University of Washington School of Medicine, 1959 NE Pacific Street, Seattle, 98195, WA, USA, phauser@u.washington.edu.
[†]currently at the Center for Molecular Biotechnology, University Torino, Torino, Italy
[*]These two authors are co-first authors of this manuscript as they contributed equally

Introduction

Membranous nephropathy, an antibody mediated and complement-dependent disease, is one of the most common forms of nephrotic syndromes in adults. Half of these patients develop progressive glomerulosclerosis, with declining renal function [1]. Although the histological hallmark is thickening of the glomerular basement membrane (from which the disease derives its name), membranous nephropathy is primarily a disease of podocytes. Podocytes are terminally differentiated epithelial cells, and injury to this cell is characterized by proteinuria. However, the precise mechanisms leading to proteinuria and the development of glomerulosclerosis in membranous nephropathy are not fully understood.

The best characterized animal model of experimental membranous nephropathy is the passive Heymann nephritis model. Disease is induced in rats by the injection of the anti-Fx1A antibody, which binds to the megalin complex of podocytes. Within 24 hours after injection the Fx1A sheep IgG binds in the subepithelial space of podocytes in a granular pattern [2]. Proteinuria is marked by day four of disease. Renal function is normal during the early stages, but deteriorates progressively over the ensuing months. Early complement activation and the resulting sublytic injury to podocytes is followed by the generation of reactive oxygen species, activation of proteases and lipid peroxidation, and increase in specific cytokines and growth factors, which all likely contribute to further tissue damage [3]. Several attempts have been made to defined potential roles for individual genes. For example protein tyrosine phosphatase receptor type O (PTPRO), Wilms' tumor gene (WT1), megalin, vascular endothelial growth factor (VEGF) have been studied following disease induction and the onset of proteinuria [4]; transcription factors and changes in matrix expression have been the focus of other studies [5–8].

While microarray studies are often dismissed as hypothesis generating, they are a very efficient technique to analyze numerous genes simultaneously and to define the complex molecular biology of pathological processes. In the field of experimental nephrology, microarray analysis has been applied to investigate several human diseases and pathological events, such as kidney tumors [9, 10], reperfusion injury [11], diabetes [12, 13] or kidney transplantation [14]. Several animal models have also been studied. Sadlier and colleagues used microarray analysis to identify changes in the transcriptome in the Thy1 model of mesangial proliferative glomerulonephritis [15]. However, a whole-genome gene expression analysis study of membranous nephropathy has not been reported.

Accordingly, to fully delineate changes in gene expression in early membranous nephropathy, we analyzed changes in the transcriptome in glomeruli by microarrays in the passive Heymann Nephritis model of membranous nephropathy prior to, and immediately following the onset of proteinuria.

Methods

Passive Heymann Nephritis (PHN) Model of Membranous Nephropathy

To induce PHN, twenty male Sprague-Dawley rats (Simson, Gilroy, CA, USA), with a bodyweight ranging from 180–200g, received a single intraperitoneal injection of sheep anti FX1A antibody (5mL/kg bodyweight) as previously described [16]. Normal sheep serum (5ml/kg) was administered to control animals. Experimental and control animals (n=5/group/time point) were sacrificed at three and six days after injections.

Measuring renal function

In order to assess proteinuria and renal function, urine was collected by placing the animals in metabolic cages for 12 hours at baseline and prior to sacrifice, during which time water was supplied without restriction [16]. Total protein excretion was determined by the sulfosalicylic acid turbidity method [17]. Creatinine excretion was measured using a colorimetric microplate assay based on the Jaffe reaction [18] (Oxford Biomedical Research, MI, USA). Animals from the experimental group were excluded if they did not develop proteinuria.

Glomerular Isolation

In order to extract RNA for the microarray analysis, glomeruli were isolated by differential sieving as previously reported [19]. Briefly, kidney cortices were removed, minced, and pressed through a series of sieves with 180μm, 106μm, and 75μm-sized mesh. Glomeruli were collected on the 75μm-sized mesh, removed from the sieve and pelleted in chilled phosphate buffered saline by centrifugation. The glomerular pellet was assessed for purity by counting the number of glomeruli and tubular fragments by microscopy. Tubular contamination was typically less then 4%.

RNA extraction, Microarray, Hybridization and Scanning

Extraction of total RNA was performed on isolated glomeruli from individual diseased and control animals by the TRIZOL® method (Invitrogene Corp, Carlsbad, CA, USA) as we have previously reported [20]. To remove potential traces of Trizol reagent, a second RNA cleanup step using Qiagen RNeasy was performed (Qiagen, Hildesheim, Germany). Quality of the isolated total RNA was checked by gel electrophoresis and with Agilent Bioanalyzer using a RNA6000 LabChip® kit (Agilent, Palo Alto, CA, USA). Quantity and OD 260/280 of total RNA and cRNA was assessed by UV spectrophotometer. cRNA was labelled with Biotin according to the Affymetrix eukaryotic target labelling protocol.

As described above, RNA was isolated from individual control and experimental animals. The RNA of two animals was pooled and hybridized on one microarray, resulting in five biological replicates at each time point (days 3 and 6) in diseased and control animals. Samples were hybridized to Affymetrix R230A GeneChip (Affymetrix, Santa Clara, CA, USA) arrays according to standard Affymetrix protocols. Quality of hybridizations and overall chip performance was determined by visual inspection of the raw scanned data. Raw data files, probe set information and files containing absolute analysis are available on: http://www.meduniwien.ac.at/nephrogene/data/index.html

Microarray analysis

Pre-processing of microarray raw data including probe-specific background correction, summarization of probe set values, and normalization was carried out with the CARMAweb (comprehensive R- and bioconductor-based web service for microarray data analysis) tool, using the robust multi-chip analysis (RMA) approach [21, 22].

The significance analysis of microarrays (SAM) method was used to identify differentially expressed genes (DEGs) between immunized rats and controls. The method calculates a set of gene-specific *t* tests followed by an estimation of the false discovery rate [23]. In our case the false discovery rate was set to < 5%. DEGs showing a fold change >1.5 were further analyzed with regard to their molecular functions, biological processes, and biological pathways using information provided by the gene ontology consortium [24], the Kyoto Encyclopaedia of Genes and Genomes (KEGG) [25], and the PANTHER (Protein ANalysis THrough Evolutionary Relationships) classification system [16]. Enriched and depleted functional categories were identified using the PANTHER data set covering the whole rat genome as reference dataset. The ratio of expected to the observed frequencies of genes assigned to certain ontology categories were compared using the χ^2 test to derive significance of differences.

Protein-protein interaction network analysis

Beginning with the set of DEGs, we generated a protein-protein interaction network following the nearest neighbour expansion method using data from the Online Predicted Human Interaction Database (OPHID) on interactions of rat proteins [26, 27]. The MCODE (Molecular Complex Detection) algorithm was used to identify highly connected subnetworks in the complete generated network [28]. The MCODE parameters *Node Score Cutoff*, *k-Core*, and *maximal depth* were set to 0.2, 2, and 100 respectively. Final identified network modules were visualized in the software environment Cytoscape [29].

Results

Proteinuria increases in PHN rats

Proteinuria measurements in PHN rats at days 3 and 6, and normal rats are shown in figure 1. As expected, proteinuria was not increased at day 3, but did increase statistically at day 6.

Patterns of Gene Expression before and after the onset of Proteinuria

Significantly differentially expressed genes (DEGs) were identified between diseased rats and control rats before (day 3) and after (day 6) the onset of proteinuria. The onset of proteinuria was detected as described earlier [16]. 55 DEGs and 225 DEGs showing fold-change values > 1.5 were detected on day three and six respectively using the SAM analysis (table 1). All DEGs showed an increase in disease compared to controls. Of the 54 DEGs detected on day three, 45 were also differentially expressed at day six.

Functional annotation of DEGs

234 genes were classified into functional groups such as cell adhesion, cell cycle, immunity and defense, transport, protein folding, developmental processes and others.

A multitude of genes were identified that encode structural proteins of the cytoskeleton or proteins required for cell adhesion such as integrin beta 1 (Itgb1), secreted phosphoprotein 1 (SPP1), laminin A (Lmna), desmin (Des), nestin (Nes), or tubulin beta 2 (Tubb2). Another functional category that was found highly enriched in increased expressed DEGs was related to cell cycle and cell proliferation. Prominent proteins such as the transforming growth factors beta 2 and 3 (TGFβ2, TGFβ3), cyclins B1 and B2 (Ccnb1, Ccnb2), or the proliferating cell nuclear antigen (PCNA) were detected in this category.

Figure 2 shows the numbers of genes that are significantly enriched in the transcriptome of PHN rats. Categories shown are significantly over-represented ($p<0.005$), the numbers within the brackets reflect the number of genes expected to be differentially regulated in the dataset. The relative numbers of genes in a certain functional group of the abundant GO terms represent the cellular processes prior to (day 3) and following the onset of proteinuria (day 6). While genes associated with cell cycle are enriched at both time points, the relative amount of cell cycle associated genes is 26.7% (or 60 genes) of all the enriched genes after the onset of proteinuria, compared to 5% beforehand. An even greater change was evident for genes with functions related to cellular immunity and defense. However, these genes are not enriched (1%) at the early time point (day 3), but at day 6 they comprise 15 % of all abundant genes (34 genes compared to 12.07 expected genes).

On day 6 the relative amount of DEGs related to cell structure and motility more increased more than two-fold from 15 genes earlier (1.82 expected genes) to 35 genes (7.6 expected) later. Changes in the relative quantity of the abundant genes between day three and day six were also detected for genes involved in developmental processes. They showed an increase

NIH-PA Author Manuscript

NIH-PA Author Manuscript

from 15 (4.16 expected) to 48 (or 17.36 expected). Table 2 gives a detailed list of the DEGs belonging to the overrepresented GO term.

Interaction modules

Four highly connected sub-networks could be identified using the MCODE algorithm integrated in the Cytoscape development environment (Figure 2). Clusters were ranked according the density of the cluster and number of nodes. Cluster 1 containing five nodes, namely Pcna, Ccnb1, Cdc2a, Gadd45a, and Gadd45g, connected through 9 interactions had the highest score based on the density and number of nodes. The proteins Itgb1, Spp1, Lgals1, and Fn1 formed the second ranked cluster (Cluster 2) as depicted in figure 3. Cluster 3 contained exclusively members of the transforming growth factor protein family, namely TGF-β2, and TGF-β3 as well as TGF-β receptors 1, 2 and 3. Cluster 4 genes were predominantly involved in cell structure and motility such as Vim, Myh9, or Myh10.

Immunostaining for Transgelin (sm22) is increased in PHN

In order to validate the microarray analysis, immunostaining was performed for the transgelin (gene with the highest mRNA increase). Figure 4 shows that transgelin staining was not detected in normal glomeruli. This was not a false negative, because transgelin staining was present in normal blood vessels, used as a positive internal control. In contrast, there was a marked increase in transgelin staining in podocytes in PHN rats. Taken together, these results validate that the protein levels were also increased, thus validating the microarray results.

Discussion

Passive Heymann Nephritis (PHN) rat model of human membranous nephropathy is characterized by proteinuria developing within 5 days after the onset of disease [5, 30–32]. To date, only inhibitors of the renin-angiotensin aldosterone system have been effective clinically at reducing proteinuria. Thus, identifying novel targets for potential therapy is needed. In this manuscript we show increases in several genes during the onset of proteinuria that may offer therapeutic targets in the future.

Changes of Gene Expression

The onset of proteinuria is marked on the transcriptome with a change in gene expression. Our results shows that prior to the onset of proteinuria (day 3 of disease), there were 54 differentially expressed genes (DEGs) in rats with membranous nephropathy compared to controls. This number increased to 225 DEGs following the onset of proteinuria (day 6 of disease). Interestingly, 44 of these DEGs were increased at both time points. Of note, transgelin (Tagln) was the single most upregulated gene showing fold-change values greater than 30. Other genes differentially regulated in our model and previously studied include Col1a1 (Collagen type 1 alpha 1) [33], Ccnb2 (cyclin B2) [31], and Actn 4 (actinin alpha 4) [4].

The relative enrichment of genes from specific functional groups, changes from day 3 to day 6. Genes involved in cell structure and motility were highly upregulated at day three (figure 2). Among the 15 genes belonging to this group were for example vimentin (Vim) or myosin heavy polypeptide 9 (Myh9).

At day six, cell cycle associated genes comprise 26.7% of all enriched genes after the onset of proteinuria (figure 2). Cell cycle proteins are induced by reactive oxygen species that contribute largely to renal injury; ROS induce DNA repair and synthesis. In PHN at day six, cellular efforts in DNA repair and synthesis are down regulated by ribonucleotide reductase

M2 (Rrm2). Rrm2 a rate limiting enzyme of DNA repair and synthesis, with a role in cell proliferation, tumorigenesis and drug resistance, is found 6.8 fold up regulated at day 6 [34]. Most of the up regulated genes are cell cycle inhibitors and cyclins that block proliferation. Cyclin kinase inhibitors were previously reported to be upregulated in experimental nephropathy [16], suggesting that podocytes are not prone to proliferate even after pronounced injury. Podocyte proliferation, like in crescentic glomerulonephritis or HIV associated nephropathy, is usually associated with rapid decline of renal function [35].

A functional group strongly overrepresented at both time points are genes involved in developmental processes (figure 2). Developmental genes represent 27.2% of all DEG at day three and 20.4% at day six. The strongest differentially regulated gene in the dataset, transgelin, is also called smooth muscle protein 22 alpha (SM22 alpha), it is a 22–25kDa actin binding protein usually associated with differentiation into smooth muscle like cell type. The mRNA coding for SM22 protein was found 70-fold upregulated at day three and 38-fold upregulated on day six (table 1). Our results also showed that the protein levels for SM22 were increased in PHN, as detected by immunostaining (figure 4). SM22 is a repressor of matrix metalloproteinase 9 (Mmp9), that functions as a type IV collagenase [36]. Mmp9 is involved in blood vessel remodelling and is involved in the proteolysis of collagen I and in the modification of platelet-derived growth factor (PDGF) [37], but more interestingly, VEGF is substrate of Mmp9. Other notable genes differentially regulated in our model that have been previously studied include Col1a1 (Collagen type 1 alpha 1) [33], Ccnb2 (cyclin B2) [31], and Actn4 (actinin alpha 4) [4].

Protein-Protein Interaction

DEGs were also screened for potential protein-protein interaction networks. 4 subnetworks could be identified (figure 3). As expected, certain of these proteins have already been studied as single proteins in glomerular injury [4, 31, 33, 38]. However, interconnections with other proteins have not been delineated and is therefore of major interest as it relates to the events in a systemic approach. The four clusters found describe the main processes in the glomerulus during the early phase of PHN coinciding and perhaps underlying the onset of proteinuria. These included: (i) DNA damage and repair genes (cluster 1); (ii) extra cellular matrix genes (cluster 2); (iii) deregulation of cytokines and growth factor genes (cluster 3); (iv) rearrangement of the cytoskeleton (cluster 4).

Cluster 1 represents the network with the highest density and the most interactions within the identified proteins (Figure 3.A). Proteins in this cluster are mainly involved in cell cycle. The five interacting proteins are Cdc2A, Ccnb1, Pcna, Gadd45a and Gadd45g. The Ccnb1 gene encodes Cyclin B1 protein. Together with Cdc2A (cell division cycle 2 protein), they form a serine/threonine kinase holoenzyme that is also known as maturation promoting factor (MPF). MPF induces the cell to undergo mitosis by phosphorylating cyclins and other cell division proteins.

The proliferation promoting action of Cdc2A and Ccnb1 as MPF is inhibited by Gadd45 (growth-arrest DNA damage-45). Gadd45 is a protein associated with DNA damage and is up-regulated in sublytic injury activated by C5b-9 [38].

When bases in the DNA are modified by reactive oxygen species (ROS), Gadd45 detects the modified sites by binding, thereby tagging them for repair. In the identified network Gadd45 interacts with Pcna (proliferating cell nuclear antigen) (Figure 3.A). Pcna has a role in DNA damage repair, as we have previously reported in this model [39]. In the current dataset Pcna was increased in PHN at day six as has been previously reported, suggesting activation of repair processes in the injured tissue [40]. Taken together, the protein-protein interactions support the hypothesis of ROS induced damage and repair. Also represented in this cluster, cell cycle inhibitory proteins are induced to prevent the cell from undergoing proliferation.

Proteins in cluster 2 (Figure 3.B) relate to extra cellular matrix proteins. One such protein is Fibronectin 1 (Fn1), is involved in many cellular processes and mechanisms like adhesion, fibrosis, cellular stress. Fn1 is increased by Tgf-β1 dependent and independent mechanism [41]. Fn1 and Tgf-β1 increase SPARC an extra cellular matrix protein, which is strongly correlated with podocyte loss due to mechanical strain [42]. Osteopontin, or Spp1 (secreted phosphoprotein 1) also present in cluster 2, is expressed in the distal tubular cells [43, 44]. Osteopontin, a protein ligand for CD44, which functions as lymphatic receptor for hyaluronic matrix proteins. Up-regulation of osteopontin in the kidney thereby influences monocyte migration into renal compartments and aggravates the immune response after the initial injury [45].

Cluster 3 demonstrates an interaction network of Tgf-β (transforming growth factor β) isoforms (Figure 3.C). Cytokines from the Tgf-β superfamily have a role in many cellular functions. Isoforms of Tgf-β are a major cause of renal fibrosis [46, 47]. We have previously reported on the differential expression of TGF-β isoforms in PHN [48]. Tgf-β has recently been shown to also induce podocyte apoptosis and reduce proliferation by limiting cell cycle progression [49]. In this model isoforms of Tgf-β were found stronger expressed after the onset of proteinuria, reflecting changes of the extra cellular matrix and complement injury.

DEGs in cluster 4 (Figure 3.D) are proteins with a structural function, some of which have a role in the cytoskeleton. For example, the extra cellular protein vimentin (Vim) was markedly increased after the onset of proteinuria. Vimentin is usually expressed in the mesenchymal tissues and upregulation suggests the early onset of mesenchymal transition of parts the glomerulus tissue. Vimentin expression is also associated in wound healing and is correlated with expression of smooth muscle proteins [50].

Myosin heavy polypeptide 9 (Myh9) is another structural protein with functions in cytoskeleton. Myh 9 encodes for myosin-IIA, a non-muscle myosin heavy chain protein. Myosin-IIA is part of the actinomyosin complex, it mediates cortical contraction in cell motility and is involved in changes of cell morphology in many cell types [51] and co-localizes with actin stress fibers [52].

Summary

The microarray data reported in this manuscript represent the serial changes in glomerular gene expression in early experimental membranous nephropathy prior to and following the onset of proteinuria. While many proteins and genes have been studied individually using other methods, profiling the full transcriptome broadens our understanding of the possible mechanisms underlying the onset and progression of PHN. Although merely descriptive in nature, microarray technology provides further insight into disease manifestation and progression, reveals novel protein interactions which serve to generate new hypotheses for further functional experiments and gives clues to potential novel therapeutic targets to modify disease.

Acknowledgments

Sources of support: This work was supported by the National Institute of Health (DK60525, DK56799, DK51096), by the American Diabetes Association and the Austrian Science Fund (Erwin Schrödinger J2415-B11 to P.H. and FWF P-15679 to R.O.). SJS is also an Established Investigator of the American Heart Association.

This work was supported by the National Institute of Health (DK60525, DK56799, DK51096), by the American Diabetes Association and Austrian Science Fund (Erwin Schrödinger J2415-B11 to P.H. and FWF P-15679 to R.O.). SJS is also an Established Investigator of the American Heart Association.

Literature

1. Cattran DC. Outcomes research in glomerulonephritis. Semin Nephrol. 2003; 23:340–354. [PubMed: 12923722]
2. Salant DJ, Darby C, Couser WG. Experimental membranous glomerulonephritis in rats. Quantitative studies of glomerular immune deposit formation in isolated glomeruli and whole animals. J Clin Invest. 1980; 66:71–81. [PubMed: 7400310]
3. Salant DJ, Belok S, Madaio MP, Couser WG. A new role for complement in experimental membranous nephropathy in rats. J Clin Invest. 1980; 66:1339–1350. [PubMed: 7440718]
4. Clement LC, Liu G, Perez-Torres I, Kanwar YS, Avila-Casado C, Chugh SS. Early changes in gene expression that influence the course of primary glomerular disease. Kidney Int. 2007; 72:337–347. [PubMed: 17457373]
5. Benigni A, Zoja C, Tomasoni S, Campana M, Corna D, Zanchi C, Gagliardini E, Garofano E, Rottoli D, Ito T, Remuzzi G. Transcriptional regulation of nephrin gene by peroxisome proliferator-activated receptor-gamma agonist: molecular mechanism of the antiproteinuric effect of pioglitazone. J Am Soc Nephrol. 2006; 17:1624–1632. [PubMed: 16687628]
6. Eddy AA. Expression of genes that promote renal interstitial fibrosis in rats with proteinuria. Kidney Int Suppl. 1996; 54:S49–54. [PubMed: 8731195]
7. Minto AW, Fogel MA, Natori Y, O’Meara YM, Abrahamson DR, Smith B, Salant DJ. Expression of type I collagen mRNA in glomeruli of rats with passive Heymann nephritis. Kidney Int. 1993; 43:121–127. [PubMed: 8433551]
8. Raats CJ, van den Born J, Bakker MA, Oppers-Walgreen B, Pisa BJ, Dijkman HB, Assmann KJ, Berden JH. Expression of agrin, dystroglycan, and utrophin in normal renal tissue and in experimental glomerulopathies. Am J Pathol. 2000; 156:1749–1765. [PubMed: 10793086]
9. Higgins JP, Shinghal R, Gill H, Reese JH, Terris M, Cohen RJ, Fero M, Pollack JR, van de Rijn M, Brooks JD. Gene expression patterns in renal cell carcinoma assessed by complementary DNA microarray. Am J Pathol. 2003; 162:925–932. [PubMed: 12598325]
10. Moch H, Schraml P, Bubendorf L, Mirlacher M, Kononen J, Gasser T, Mihatsch MJ, Kallioniemi OP, Sauter G. High-throughput tissue microarray analysis to evaluate genes uncovered by cDNA microarray screening in renal cell carcinoma. Am J Pathol. 1999; 154:981–986. [PubMed: 10233835]
11. Perco P, Pleban C, Kainz A, Lukas A, Mayer B, Oberbauer R. Gene expression and biomarkers in renal transplant ischemia reperfusion injury. Transpl Int. 2007; 20:2–11. [PubMed: 17181647]
12. Baelde HJ, Eikmans M, Doran PP, Lappin DW, de Heer E, Bruijn JA. Gene expression profiling in glomeruli from human kidneys with diabetic nephropathy. Am J Kidney Dis. 2004; 43:636–650. [PubMed: 15042541]
13. Susztak K, Bottinger E, Novetsky A, Liang D, Zhu Y, Ciccone E, Wu D, Dunn S, McCue P, Sharma K. Molecular profiling of diabetic mouse kidney reveals novel genes linked to glomerular disease. Diabetes. 2004; 53:784–794. [PubMed: 14988265]
14. Hauser P, Schwarz C, Mitterbauer C, Regele HM, Muhlbacher F, Mayer G, Perco P, Mayer B, Meyer TW, Oberbauer R. Genome-wide gene-expression patterns of donor kidney biopsies distinguish primary allograft function. Lab Invest. 2004; 84:353–361. [PubMed: 14704720]
15. Sadlier DM, Ouyang X, McMahon B, Mu W, Ohashi R, Rodgers K, Murray D, Nakagawa T, Godson C, Doran P, Brady HR, Johnson RJ. Microarray and bioinformatic detection of novel and established genes expressed in experimental anti-Thy1 nephritis. Kidney Int. 2005; 68:2542–2561. [PubMed: 16316330]
16. Shankland SJ, Floege J, Thomas SE, Nangaku M, Hugo C, Pippin J, Henne K, Hockenberry DM, Johnson RJ, Couser WG. Cyclin kinase inhibitors are increased during experimental membranous nephropathy: potential role in limiting glomerular epithelial cell proliferation in vivo. Kidney Int. 1997; 52:404–413. [PubMed: 9263996]

17. Davidson, I.; Henry, JB. Clinical Diagnosis by Laboratory Methods. 19. Philadelphia: Saunders; 1969. p. 48
18. Slot C. Plasma creatinine determination. A new and specific Jaffe reaction method. Scand J Clin Lab Invest. 1965; 17:381–387. [PubMed: 5838275]
19. Ohse T, Pippin JW, Vaughan MR, Brinkkoetter PT, Krofft RD, Shankland SJ. Establishment of conditionally immortalized mouse glomerular parietal epithelial cells in culture. J Am Soc Nephrol. 2008; 19:1879–1890. [PubMed: 18596122]
20. Petermann AT, Hiromura K, Blonski M, Pippin J, Monkawa T, Durvasula R, Couser WG, Shankland SJ. Mechanical stress reduces podocyte proliferation in vitro. Kidney Int. 2002; 61:40–50. [PubMed: 11786083]
21. Irizarry RA, Bolstad BM, Collin F, Cope LM, Hobbs B, Speed TP. Summaries of Affymetrix GeneChip probe level data. Nucleic Acids Res. 2003; 31:e15. [PubMed: 12582260]
22. Rainer J, Sanchez-Cabo F, Stocker G, Sturn A, Trajanoski Z. CARMAweb: comprehensive R- and bioconductor-based web service for microarray data analysis. Nucleic Acids Res. 2006; 34:W498–W503. [PubMed: 16845058]
23. Tusher VG, Tibshirani R, CHu G. Significance analysis of microarrays applied to the ionizing radiation response. Proc Natl Acad Sci U S A. 2001; 98:5116–5121. [PubMed: 11309499]
24. Ashburner M, Ball CA, Blake JA, Botstein D, Butler H, Cherry JM, Davis AP, Dolinski K, Dwight SS, Eppig JT, Harris MA, Hill DP, Issel-Tarver L, Kasarskis A, Lewis S, Matese JC, Richardson JE, Ringwald M, Rubin GM, Sherlock G. Gene ontology: tool for the unification of biology. The Gene Ontology Consortium. Nat Genet. 2000; 25:25–29. [PubMed: 10802651]
25. Kanehisa M, Goto S. KEGG: kyoto encyclopedia of genes and genomes. Nucleic Acids Res. 2000; 28:27–30. [PubMed: 10592173]
26. Chen JY, Shen C, Sivachenko AY. Mining Alzheimer disease relevant proteins from integrated protein interactome data. Pac Symp Biocomput. 2006:367–378. [PubMed: 17094253]
27. Brown KR, Jurisica I. Online predicted human interaction database. Bioinformatics. 2005; 21:2076–2082. [PubMed: 15657099]
28. Bader GD, Hogue CW. An automated method for finding molecular complexes in large protein interaction networks. BMC Bioinformatics. 2003; 4:2. [PubMed: 12525261]
29. Shannon P, Markiel A, Ozier O, Baliga NS, Wang JT, Ramage D, Amin N, Schwikowski B, Ideker T. Cytoscape: a software environment for integrated models of biomolecular interaction networks. Genome Res. 2003; 13:2498–2504. [PubMed: 14597658]
30. Nakatsue T, Koike H, Han GD, Suzuki K, Miyauchi N, Yuan H, Salant DJ, Gejyo F, Shimizu F, Kawachi H. Nephrin and podocin dissociate at the onset of proteinuria in experimental membranous nephropathy. Kidney Int. 2005; 67:2239–2253. [PubMed: 15882266]
31. Nangaku M, Shankland SJ, Couser WG. Cellular response to injury in membranous nephropathy. J Am Soc Nephrol. 2005; 16:1195–1204. [PubMed: 15800119]
32. Saran AM, Yuan H, Takeuchi E, McLaughlin M, Salant DJ. Complement mediates nephrin redistribution and actin dissociation in experimental membranous nephropathy. Kidney Int. 2003; 64:2072–2078. [PubMed: 14633129]
33. Bonegio RG, Fuhro R, Wang Z, Valeri CR, Andry C, Salant DJ, Lieberthal W. Rapamycin ameliorates proteinuria-associated tubulointerstitial inflammation and fibrosis in experimental membranous nephropathy. J Am Soc Nephrol. 2005; 16:2063–2072. [PubMed: 15917339]
34. Zhou B, Yen Y. Characterization of the human ribonucleotide reductase M2 subunit gene; genomic structure and promoter analyses. Cytogenet Cell Genet. 2001; 95:52–59. [PubMed: 11978970]
35. Griffin SV, Krofft RD, Pippin JW, Shankland SJ. Limitation of podocyte proliferation improves renal function in experimental crescentic glomerulonephritis. Kidney Int. 2005; 67:977–986. [PubMed: 15698436]
36. Nair RR, Solway J, Boyd DD. Expression cloning identifies transgelin (SM22) as a novel repressor of 92-kDa type IV collagenase (MMP-9) expression. J Biol Chem. 2006; 281:26424–26436. [PubMed: 16835221]
37. Page-McCaw A, Ewald AJ, Werb Z. Matrix metalloproteinases and the regulation of tissue remodelling. Nat Rev Mol Cell Biol. 2007; 8:221–233. [PubMed: 17318226]

38. Pippin JW, Durvasula R, Petermann A, Hiromura K, Couser WG, Shankland SJ. DNA damage is a novel response to sublytic complement C5b-9-induced injury in podocytes. J Clin Invest. 2003; 111:877–885. [PubMed: 12639994]

39. Hiromura K, Haseley LA, Zhang P, Monkawa T, Durvasula R, Petermann AT, Alpers CE, Mundel P, Shankland SJ. Podocyte expression of the CDK-inhibitor p57 during development and disease. Kidney Int. 2001; 60:2235–2246. [PubMed: 11737597]

40. Xia L, Zheng L, Lee HW, Bates SE, Federico L, Shen B, O'Connor TR. Human 3- methyladenine-DNA glycosylase: effect of sequence context on excision, association with PCNA, and stimulation by AP endonuclease. J Mol Biol. 2005; 346:1259–1274. [PubMed: 15713479]

41. Yung S, Lee CY, Zhang Q, Lau SK, Tsang RC, Chan TM. Elevated glucose induction of thrombospondin-1 up-regulates fibronectin synthesis in proximal renal tubular epithelial cells through TGF-beta1 dependent and TGF-beta1 independent pathways. Nephrol Dial Transplant. 2006; 21:1504–1513. [PubMed: 16495290]

42. Durvasula RV, Shankland SJ. Mechanical strain increases SPARC levels in podocytes: implications for glomerulosclerosis. Am J Physiol Renal Physiol. 2005; 289:F577–584. [PubMed: 16093428]

43. Kohri K, Nomura S, Kitamura Y, Nagata T, Yoshioka K, Iguchi M, Yamate T, Umekawa T, Suzuki Y, Sinohara H. Structure and expression of the mRNA encoding urinary stone protein (osteopontin). J Biol Chem. 1993; 268:15180–15184. [PubMed: 8325891]

44. Kohri K, Suzuki Y, Yoshida K, Yamamoto K, Amasaki N, Yamate T, Umekawa T, Iguchi M, Sinohara H, Kurita T. Molecular cloning and sequencing of cDNA encoding urinary stone protein, which is identical to osteopontin. Biochem Biophys Res Commun. 1992; 184:859–864. [PubMed: 1575754]

45. Yu XQ, Nikolic-Paterson DJ, Mu W, Giachelli CM, Atkins RC, Johnson RJ, Lan HY. A functional role for osteopontin in experimental crescentic glomerulonephritis in the rat. Proc Assoc Am Physicians. 1998; 110:50–64. [PubMed: 9460083]

46. Border WA, Noble NA. Transforming growth factor beta in tissue fibrosis. N Engl J Med. 1994; 331:1286–1292. [PubMed: 7935686]

47. Border WA, Okuda S, Languino LR, Sporn MB, Ruoslahti E. Suppression of experimental glomerulonephritis by antiserum against transforming growth factor beta1. Nature. 1990; 346:371–374. [PubMed: 2374609]

48. Shankland SJ, Pippin J, Pichler RH, Gordon KL, Friedman S, Gold LI, Johnson RJ, Couser WG. Differential expression of transforming growth factor-beta isoforms and receptors in experimental membranous nephropathy. Kidney Int. 1996; 50:116–124. [PubMed: 8807580]

49. Schiffer M, Bitzer M, Roberts IS, Kopp JB, ten Dijke P, Mundel P, Bottinger EP. Apoptosis in podocytes induced by TGF-beta and Smad7. J Clin Invest. 2001; 108:807–816. [PubMed: 11560950]

50. Ivanova L, Butt MJ, Matsell DG. Mesenchymal Transition in Kidney Collecting Duct Epithelial Cells. Am J Physiol Renal Physiol. 2008

51. van Leeuwen FN, van Delft S, Kain HE, van der Kammen RA, Collard JG. Rac regulates phosphorylation of the myosin-II heavy chain, actinomyosin disassembly and cell spreading. Nat Cell Biol. 1999; 1:242–248. [PubMed: 10559923]

52. Takubo T, Wakui S, Daigo K, Kurokata K, Ohashi T, Katayama K, Hino M. Expression of non-muscle type myosin heavy polypeptide 9 (MYH9) in mammalian cells. Eur J Histochem. 2003; 47:345–352. [PubMed: 14706930]

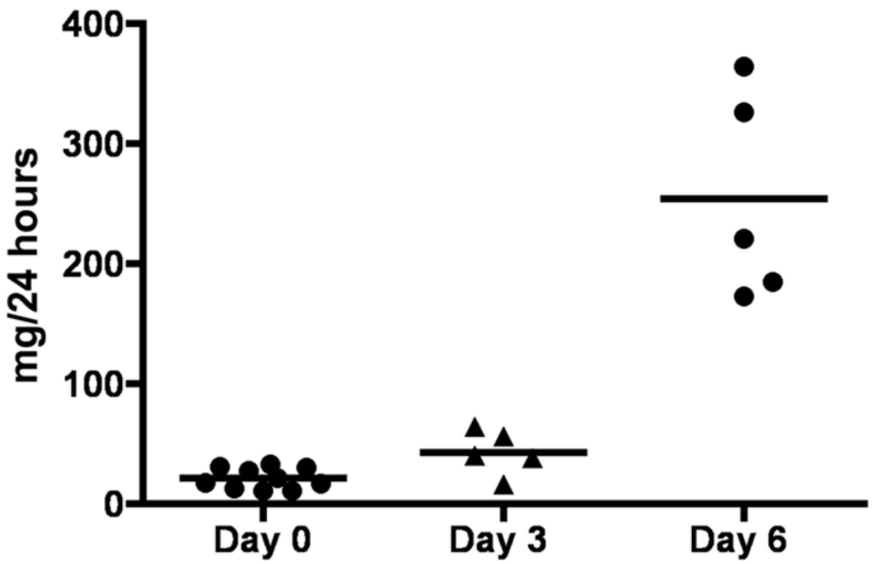

Figure 1. Proteinuria

Graph in figure 1 is showing total protein excretion of rats at the baseline (day 0) and after induction of disease (day 3 and day 6).

NIH-PA Author Manuscript
NIH-PA Author Manuscript

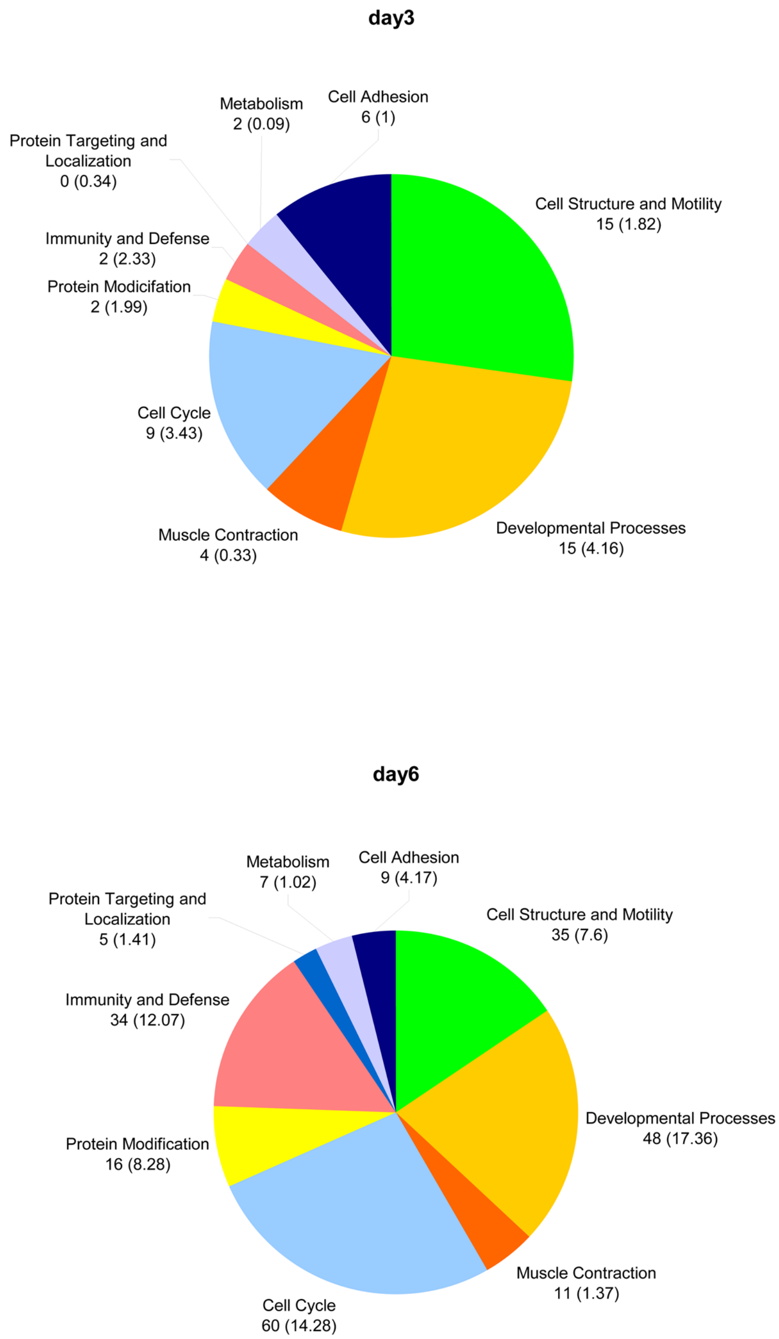

Figure 2. Enriched biological processes

Enriched biological processes and number of differentially expressed genes are given in figure 2. Numbers in brackets depict expected gene numbers according to the background distribution of all human genes.

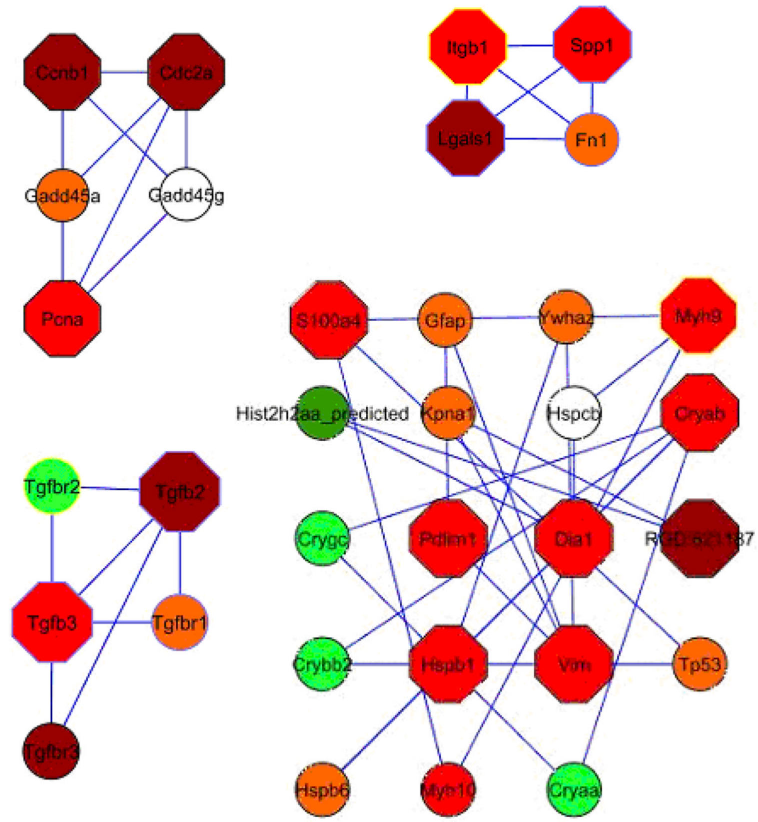

Figure 3. Protein interaction modules

Graphical visualization of the top four network modules. Node fill colour indicates the measured fold-change, where green represents down regulated genes (light green < −1.5, dark green < −2) and red represents upregulated genes (orange <1.5, red >1.5, dark red >2). The node's border colour indicates the subcellular localization of the protein (yellow for membrane and blue for extra cellular). Hexagon shape of the node represents DEGs and circular shape represents direct interacting proteins.

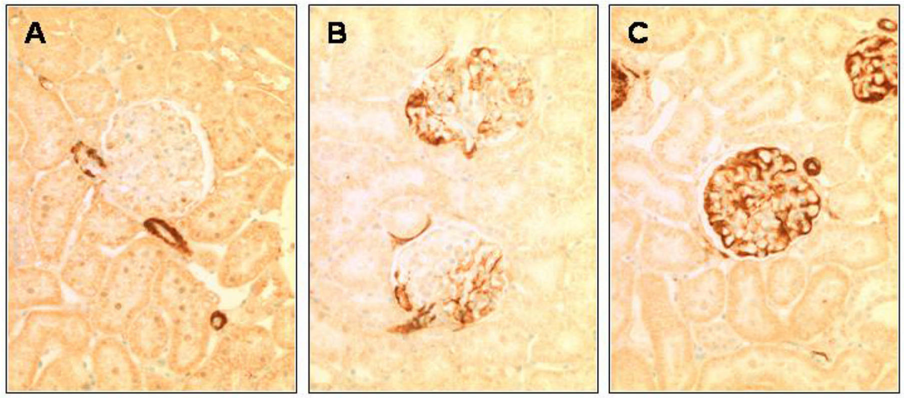

Figure 4. SM22 levels in PHN

(A) Staining for SM22 is absent in control glomeruli, but is detected in the blood vessels. (B) SM22 staining is detected in the glomerulus at day 3 of PHN, in a podocyte distribution. (C) SM22 staining is markedly increased at day 6 of PHN in podocytes. Staining was absent when the primary antibody was omitted (not shown).

Table 1

Differentially expressed genes (DEGs)

	Symbol	Gene Name	Fold Change	
			Day 3	Day 6
Apoptosis				
BE112895	Pea15 *	phosphoprotein enriched in astrocytes 15		2.55
AI411997	Adamtsl4	ADAMTS-like 4		1.90
NM_012935	Cryab	crystallin, alpha B		1.75
NM_022546	Dapk3	death-associated protein kinase 3	1.51	1.54
BF282636	RGD1305457	similar to RIKEN cDNA 1700023M03		1.54
NM_017180	Phlda1	pleckstrin homology-like domain, family A, member 1		1.50
Cell Adhesion				
Z78279	Col1a1	collagen, type 1, alpha 1	7.68	14.09
AF056034	Nexn	nexilin	4.77	4.55
BI303379	Tnfrsf12	tumor necrosis factor receptor superfamily, member 12a	3.70	4.21
BF407194	Itgb1bp2 *	integrin beta 1 binding protein 2	2.14	2.09
NM_030828	Gpc1	glypican 1		2.02
NM_017022	Itgb1	integrin beta 1		1.82
NM_012811	Mfge8	milk fat globule-EGF factor 8 protein		1.79
BG379319	Tgfbi	transforming growth factor, beta induced		1.72
NM_022266	Ctgf	connective tissue growth factor		1.66
AW433888	Vcl *	vinculin		1.63
NM_133409	Ilk	integrin linked kinase	1.52	1.61
BI275904	Lims2 *	LIM and senescent cell antigen like domains 2	1.63	1.59
AI008975	LOC311772	similar to nidogen 2		1.57
NM_022523	Cd151	CD151 antigen		1.51
NM_019237	Pcolce	procollagen C-proteinase enhancer protein		1.50
AB001382	Spp1	secreted phosphoprotein 1	2.10	
NM_012774	Gpc3	glypican 3	1.87	
Cell Structure and Motility				
U22520	Cxcl10	chemokine (C-X-C motif) ligand 10		3.66
BE111697	Kif20a *	kinesin family member 20A		3.55

NIH-PA Author Manuscript
NIH-PA Author Manuscript

	Symbol	Gene Name	Fold Change	
			Day 3	Day 6
NM_022531	Des	desmin	1.85	3.29
NM_031005	Actn1	actinin, alpha 1	3.00	3.19
BI283060	Flna *	filamin, alpha	2.60	2.96
NM_019131	Tpm1	tropomyosin 1, alpha	3.33	2.90
BI279044	Myl9 *	myosin, light polypeptide 9, regulatory	5.58	2.81
AI179391	Enh	enigma homolog	2.04	2.58
NM_017148	Csrp1	cysteine and glycine-rich protein 1	1.92	2.42
X03369	Tubb2b	tubulin, beta 2b		2.34
BI274903	RGD1305887 *	similar to RIKEN cDNA 2310057H16	1.80	2.27
AA012755	MGC109519	similar to tropomyosin 1, embryonic fibroblast - rat		2.23
NM_019361	Arc	activity regulated cytoskeletal-associated protein		2.18
NM_012987	Nes	nestin		2.07
AI598442	RGD1564875 *	similar to mKIAA0613 protein		2.04
AW919109	Cap2	CAP, adenylate cyclase-associated protein, 2 (S. cerevisiae)	1.88	2.03
BI285440	Tubb5	tubulin, beta 5		1.91
AI103106	Lmnb1	lamin B1		1.86
AA892044	Tubb2	tubulin, beta, 2		1.80
NM_013194	Myh9	myosin, heavy polypeptide 9		1.76
NM_031970	Hspb1	heat shock 27kDa protein 1		1.74
BG381583	RGD1565118 *	similar to mKIAA0843 protein		1.68
X70706	Pls3	plastin 3 (T-isoform)		1.67
BM391364	LOC290704		1.60	1.67
BI296011	Cfl2 *	cofilin 2, muscle		1.65
NM_021755	Lmna	lamin A		1.63
NM_130411	Coro1a	coronin, actin binding protein 1A		1.63
BI278813	Ckap4 *	cytoskeleton-associated protein 4		1.60
BM383953	LOC367171	microtubule-associated protein 4		1.57
NM_031675	Actn4	actinin alpha 4	1.51	1.56
AA891834	Col4a5 *	collagen, type IV, alpha 5		1.56
AI407239	Myom2	myomesin 2		1.55

NIH-PA Author Manuscript
NIH-PA Author Manuscript

	Symbol	Gene Name	Fold Change	
			Day 3	Day 6
NM_031140	Vim	vimentin		1.54
NM_134452	Col5a1	collagen, type V, alpha 1		1.52
AI180161	Mapre1	microtubule-associated protein, RP/EB family, member 1		1.52
AW252250	Nebl *	nebulette		1.51
NM_019212	Acta1	actin, alpha 1, skeletal muscle	6.03	
Cell Cycle				
BG379338	Rrm2	ribonucleotide reductase M2		6.87
BE113362	Cdkn3 *	cyclin-dependent kinase inhibitor 3		5.53
AI409259	Racgap1 *	Rac GTPase-activating protein 1		5.02
AA944180	RGD1562047 *	similar to Cyclin-dependent kinases regulatory subunit 2 (CKS-2)		5.00
NM_019296	Cdc2a	cell division cycle 2 homolog A (S. pombe)		4.40
AW253821	Ccnb2 *	cyclin B2		3.47
BI296084	Ube2c *	ubiquitin-conjugating enzyme E2C		3.15
NM_031131	Tgfb2	transforming growth factor, beta 2	2.06	3.06
NM_021989	Timp2	tissue inhibitor of metalloproteinase 2	1.58	2.44
BF417638	RGD:1359093	similar to cell division cycle associated 3		2.27
BG380355	Cdca8	cell division cycle associated 8		2.24
U05341	Cdc20	cell division cycle 20 homolog (S. cerevisiae)		2.20
BE117002	LOC362021			2.12
AI408269	Spbc25	spindle pole body component 25 homolog (S. cerevisiae)		2.06
NM_053483	Kpna2	karyopherin (importin) alpha 2		2.04
AA874827	Dlg7 *	discs, large homolog 7 (Drosophila)		1.84
AA996882	Stk6	serine/threonine kinase 6		1.82
AW920000	LOC362587	similar to microfilament and actin filament cross-linker protein isoform b		1.81
NM_022381	Pcna	proliferating cell nuclear antigen		1.78
X64589	Ccnb1	cyclin B1		1.72
AI407985	LOC686524	hypothetical protein LOC686524		1.70
AF140232	S100a6	S100 calcium binding protein A6 (calcyclin)		1.69
BM386384	Nap1l1	nucleosome assembly protein 1-like 1		1.65
NM_053819	Timp1	Tissue inhibitor of metalloproteinase 1		2.30

	Symbol	Gene Name	Fold Change	
			Day 3	Day 6
AA957183	Cit	citron		1.57
NM_013174	Tgfb3	transforming growth factor, beta 3		1.55
Immunity and Defense				
AI233530	C1qtnf3 *	C1q and tumor necrosis factor related protein 3		2.67
BI284441	Colec12	collectin sub-family member 12		2.59
BI278802	Prnp	prion protein		2.51
BF389535	LOC299339	similar to Tumor necrosis factor, alpha-induced protein 2 (primary response gene B94)		2.14
NM_053843	Fcgr3	Fc receptor, IgG, low affinity III		2.10
AI176519	Ier3	immediate early response 3		2.08
L12458	Lyz	lysozyme		2.05
AW918311	C1qtnf4 *	C1q and tumor necrosis factor related protein 4		2.02
NM_012620	Serpine1	serine (or cysteine) proteinase inhibitor, clade E, member 1		1.66
AI228623	Nptx2 *	neuronal pentraxin II		1.64
NM_031971	Hspa1a	heat shock 70kD protein 1A		1.54
Transport (membrane)				
BI293600	Slc35b2	solute carrier family 35, member B2	2.08	2.64
NM_019354	Ucp2	uncoupling protein 2		1.50
Transport (intracellular)				
NM_022959	Pamci	peptidylglycine alpha-amidating monooxygenase COOH-terminal interactor		1.57
BG381589	Stx6	syntaxin 6		1.50
Transport (other)				
AI170609	RGD1560252 *	similar to hypothetical protein MGC31967	4.02	3.10
AI407838	Ecm1	extracellular matrix protein 1		2.04
NM_022278	Glrx1	glutaredoxin 1 (thioltransferase)		1.52
BE111722	Ndufs2 *	NADH dehydrogenase (ubiquinone) Fe-S protein 2		1.52
Metabolism (lipid)				
NM_031043	Gyg1	glycogenin 1	1.59	2.64
NM_013200	Cpt1b	carnitine palmitoyltransferase 1b	1.60	2.43
AF248543	A3galt2	alpha 1,3-galactosyltransferase 2 (isoglobotriaosylceramide synthase)		1.74
NM_017235	Hsd17b7	hydroxysteroid (17-beta) dehydrogenase 7		1.67

NIH-PA Author Manuscript
NIH-PA Author Manuscript

	Symbol	Gene Name	Fold Change	
			Day 3	Day 6
NM_012941	Cyp51	cytochrome P450, subfamily 51		1.67
NM_031840	Fdps	farensyl diphosphate synthase		1.51
Metabolism (glycogen)				
AW919180	Pygm	muscle glycogen phosphorylase	1.85	1.76
Metabolism (DNA)				
NM_022674	H2afz	H2A histone family, member Z		1.61
Metabolism (other)				
AA891760	RGD1308350 *	similar to hypothetical protein MGC13251		1.68
BG381486	Large *	like-glycosyltransferase		1.64
BM385390	Uxs1	UDP-glucuronate decarboxylase 1		1.58
BI282076	Prdx4	peroxiredoxin 4		1.52
Protein Modification				
AI236997	Dusp14 *	dual specificity phosphatase 14		2.24
NM_130403	Ppp1r14a	protein phosphatase 1, regulatory (inhibitor) subunit 14A		1.82
AW531714	Ube2t *	ubiquitin-conjugating enzyme E2T (putative)		1.76
BI276525	Ate1 *	arginine-tRNA-protein transferase 1		1.70
BI283703	Mapkapk2	MAP kinase-activated protein kinase 2		1.69
AF106659	Usp2	ubiquitin specific protease 2		1.68
NM_053323	Degs	degenerative spermatocyte homolog (Drosophila)		1.64
AI010241	Usp1 *	ubiquitin specific protease 1		1.63
AA799400	B3galt3 *	UDP-Gal:betaGlcNAc beta 1,3-galactosyltransferase, polypeptide 3		1.59
AA849399	Ctsz	cathepsin Z		1.54
BI279788	Ube2s *	ubiquitin-conjugating enzyme E2S		1.51
NM_024135	Limk2	LIM motif-containing protein kinase 2		1.50
Protein Folding				
AI175031	Dnajb4 *	DnaJ (Hsp40) homolog, subfamily B, member 4		1.53
BG671521	Hspca	heat shock protein 1, alpha		1.54
Signal Transduction				
NM_019904	Lgals1	lectin, galactose binding, soluble 1	1.61	3.71
NM_012715	Adm	adrenomedullin	1.78	2.86

	Symbol	Gene Name	Fold Change	
			Day 3	Day 6
BF405151	Gpr39 *	G protein-coupled receptor 39	1.72	2.80
NM_053634	Fcnb	ficolin B	1.91	2.70
NM_033099	Ptprv	protein tyrosine phosphatase, receptor type, V		2.27
BE117002	RGD1560967 *	similar to Pins		2.12
AW253242	Magi1 *	membrane associated guanylate kinase interacting protein-like 1		1.74
X78595	Npr3	natriuretic peptide receptor 3		1.74
BG378926	S100a11	S100 calcium binding protein A11 (calizzarin)		1.73
BI276015	RGD1559882 *	similar to hypothetical protein E130310N06		1.66
BM386204	Ran	RAN, member RAS oncogene family		1.65
BI295991	Rab2l	RAB2, member RAS oncogene family-like		1.60
NM_022236	Pde10a	phosphodiesterase 10A	1.56	1.56
NM_012823	Anxa3	annexin A3		1.51
NM_053299	Ubd	ubiquitin D	1.72	
M35297	Mrgprf	MAS-related GPR, member F	1.79	
Transcription				
BM385445	Top2a	topoisomerase (DNA) 2 alpha		3.37
L81174	Ankrd1	ankyrin repeat domain 1 (cardiac muscle)	2.62	3.02
NM_031628	Nr4a3	nuclear receptor subfamily 4, group A, member 3		2.34
NM_017187	Hmgb2	high mobility group box 2		2.04
NM_131902	Cdkn2c	cyclin-dependent kinase inhibitor 2C (p18, inhibits CDK4)		2.01
NM_017365	Pdlim1	PDZ and LIM domain 1 (elfin)		2.00
AI170362	Nfkb2	nuclear factor of kappa light polypeptide gene enhancer in B-cells 2, p49/p100		1.95
U17565	Mcmd6	mini chromosome maintenance deficient 6 (S. cerevisiae)		1.88
NM_053583	Zfp423	zinc finger protein 423		1.87
BM387864	Lrrfip1	similar to FLI-LRR associated protein-1		1.76
BG664147	Ptrf *	polymerase I and transcript release factor		1.65
BG380385	Srf *	serum response factor	1.95	1.64
BF403027	Hdac5	histone deacetylase 5		1.64
AI179264	Creb3	cAMP responsive element binding protein 3		1.50
Homeostasis				

	Symbol	Gene Name	Fold Change	
			Day 3	Day 6
BI285437	Nxn *	nucleoredoxin		1.62
Nucleus				
BE104102	RGD1306774 *	similar to SPT3-associated factor 42		1.83
Membrane				
BM385031	Plp2	proteolipid protein 2	1.76	2.55
BM388441	RGD1311946 *	similar to RIKEN cDNA 1810055G02		1.97
NM_030847	Emp3	epithelial membrane protein 3		1.89
AW917760	RGD1564216 *	similar to Myoferlin (Fer-1 like protein 3)		1.88
AI009530	MGC72614	hypothetical LOC310540		1.86
BI296048	Myadm	myeloid-associated differentiation marker	1.55	1.77
J03867	Dia1	diaphorase 1		1.60
BM385463	Tmem43	transmembrane protein 43		1.55
AI230273	RGD:735199	Unknown (protein for MGC:72987)		1.55
BF283798	Nipsnap3a	nipsnap homolog 3A (C. elegans)		1.53
AA850909	Pvrl2 *	poliovirus receptor-related 2 (herpesvirus entry mediator B)		1.50
BI290029	RGD1562920 *	similar to Aig1 protein		1.50
AI407016	RGD1307736 *	similar to Hypothetical protein KIAA0152	1.55	
BI294974	Ldlr	low density lipoprotein receptor	1.69	
Developmental Processes				
NM_031549	Tagln	transgelin	69.77	38.66
NM_012636	Pthlh	parathyroid hormone-like peptide		3.13
NM_030584	Sost	sclerostin		3.12
AW141680	Bmp6	bone morphogenetic protein 6		2.36
NM_019242	Ifrd1	interferon-related developmental regulator 1	2.05	2.32
AW251450	Mustn1	musculoskeletal, embryonic nuclear protein 1		2.13
AI235465	Ssg1	steroid sensitive gene 1		2.07
AW435036	Smtn *	smoothelin		1.65
BI290551	Fnbp1	Formin binding protein 1		1.60
BI275485	Sema3b *	semaphorin 3B, immunoglobulin domain, secreted		1.57
AW144216	Enpep	glutamyl aminopeptidase	2.11	1.57

NIH-PA Author Manuscript
NIH-PA Author Manuscript

	Symbol	Gene Name	Fold Change	
			Day 3	Day 6
BG666787	Gmfg	glia maturation factor, gamma		1.56
BM384088	Socs2	suppressor of cytokine signaling 2		1.54
NM_031114	S100a10	S100 calcium binding protein A10 (calpactin)		1.51
Others				
AI229404	RGD1566097 *	similar to Anillin	2.47	8.41
BI295828			2.28	3.31
BI279587			2.12	3.01
BI283695			1.73	2.48
AW531909				2.44
BF419834			1.62	2.29
BF415061	RGD1307034 *	similar to hypothetical protein CG003		2.21
BF408518	RGD1305081 *	similar to ionized calcium binding adapter molecule 2 (Iba2)	1.98	2.16
AI712694	RGD1308747 *	similar to hypothetical protein FLJ10156		2.15
BI296728	RGD1564957 *	similar to RIKEN cDNA 3110007P09		2.04
AI176172				2.03
BM387112			1.71	2.03
AI071000				2.00
AA799328	RGD1560913 *	similar to expressed sequence AW413625		1.93
BE096535		transcribed locus, strongly similar to XP_574462.1 similar to hypoth. protein C230069C04		1.89
BG378155	RGD1565079 *	similar to hypothetical protein MGC17839		1.88
AA943808	RGD1307215	similar to protein phosphatase 1, inhibitory subunit 1C; thymocyte ARPP		1.82
AW143197				1.79
AW529960				1.78
AI177743	LOC498261			1.72
AI317841	Gramd3	GRAM domain containing 3		1.69
BI303106				1.64
BF561368	RGD1306959 *	similar to C11orf17 protein		1.63
AW253004		CDNA clone IMAGE:7317367		1.62
BF398756				1.62
AI009167	Zfp451 *	zinc finger protein 451		1.62

	Symbol	Gene Name	Fold Change	
			Day 3	Day 6
AI412389				1.61
BE111057				1.60
BI282694	RGD1565037 *	similar to selenoprotein SelM		1.60
AI231225				1.58
AA942716	Hn1	hematological and neurological expressed sequence 1		1.56
BF284519				1.55
BG671786				1.53
AW914928				1.53
AI113146	Acpl2	acid phosphatase-like 2		1.51
AI170820	RGD1310383 *	similar to T-cell activation protein phosphatase 2C		1.50
AA800892	RGD1563599 *	similar to putative SH3BGR protein	1.81	
BG380430	RGD1564105 *	similar to RIKEN cDNA B130052G07	1.54	
NM_021584	Ania4	activity and neurotransmitter-induced early gene protein 4 (ania-4)		2.53
AA997359	Serpinb6	serine (or cysteine) peptidase inhibitor, clade B, member 6		1.54
NM_012618	S100a4	S100 calcium-binding protein A4		1.80
NM_022382	Pde4dip	phosphodiesterase 4D interacting protein (myomegalin)		1.70
AI112962	Rcn *	reticulocalbin		1.92
AI232065	Arhgap18 *	Rho GTPase activating protein 18		1.55

List of 234 differentially regulated genes (>1.5 fold) in PHN induced rats on day three and or day six. Genes are annotated with NCBI Gene Symbols and grouped according to biological function. Starred (*) Gene Symbols mark predicted genes.

NIH-PA Author Manuscript
NIH-PA Author Manuscript

Table 2

List of over- and underrepresented ontology terms in the dataset

	day 3			day 6		
	genes	over/under	p-value	genes	over/under	p-value
Biological Processes						
Cell structure and motility	15	+	4.20E-010	35	+	1.02E-013
-Cell structure	12	+	1.33E-009	27	+	3.08E-013
-Cell motility	6	+	3.74E-005	17	+	9.07E-010
Developmental processes	11	+	1.46E-003	36	+	9.29E-007
-Mesoderm development	4	/	/	15	+	2.68E-005
Cell cycle	3	/	/	27	+	2.29E-010
-Mitosis	3	/	/	10	+	2.53E-004
-Cell cycle control	1	/	/	10	+	1.01E-003
Muscle contraction	4	+	4.29E-004	11	+	2.30E-007
Immunity and defense	2	/	/	21	+	4.34E-004
-Macrophage-mediated immunity	0	/	/	5	+	1.81E-003
-Stress response	0	/	/	8	+	1.86E-004
Tumor supressor	1	/	/	5	+	4.73E-004
Metabolism			/			
- sulfur redox	0	/	/	2	+	1.23E-002
- glycogen	2	+	3.84E-003	2	/	/
Cell adhesion	6	+	6.59E-004	9	/	/
G-protein mediated signaling	1	/	/	2	−	1.11E-002
Protein modification	2	/	/	16	+	1.14E-002
Molecular Function						
Cytoskeletal protein	15	+	4.58E-012	37	+	1.14E-019
-Actin binding cytoskeletal protein	12	+	2.10E-012	23	+	5.29E-015
-Microtuble family cytoskeletal protein	2	/	/	7	+	1.58E-003
-Intermediate filament	1	/	/	5	+	1.05E-003
Non-motor actin binding protein	4	+	2.35E-004	11	+	4.73E-008
Actin binding motor protein	1	/	/	3	+	7.30E-003
Tubulin	2	+	1.37E-003	4	+	7.37E-005

	day 3			day 6		
	genes	over/under	p-value	genes	over/under	p-value
Select regulatory molecule	2	/	/	22	+	3.87E-005
-Kinase modulator	1	/	/	7	+	1.99E-004
Metalloprotease inhibitor	1	+	8.26E-003	2	+	5.35E-004
Miscellaneous function	5	/	/	14	+	2.49E-003
-Structural protein	2	/	/	8	+	1.01E-004
Signaling molecule	4	/	/	16	+	2.29E-004
-Growth factor	1	/	/	4	+	1.30E-002
Defense/Immunity protein	2	/	/	8	+	6.04E-003
Non-receptor serine/threonine kinase	2	/	/	7	+	8.53E-003
Select calcium binding protein	1	/	/	8	+	1.15E-003
-Calmodulin related protein	1	/	/	6	+	1.01E-003
G-protein coupled receptor	1	/	/	0	−	2.09E-003
Nucleic acid binding	2	/	/	9	−	1.16E-002
PANTHER pathways						
Integrin signaling pathway	6	+	3.88E-006	10	+	8.61E-006
Cytoskeletal regulation by Rho GTPase	2	/	/	7	+	1.97E-005
Hedgehog signaling pathway	2	+	3.35E-003	4	+	4.14E-004
p53 pathway	0	/	/	5	+	2.31E-003
DNA replication	0	/	/	2	+	1.00E-002
KEGG pathways						
Focal adhesion	6			9		
Cell cycle	1			9		
Regulation of actin cytoskeleton	3			8		
MAPK signaling pathway	3			7		
Cell communication	2			7		
Leukocyte transendothelial migration	3			5		
Gap junction	2			5		
axon guidance	0			5		
Tight junction	3			4		
Adherens junction	2			4		

NIH-PA Author Manuscript
NIH-PA Author Manuscript

	day 3			day 6		
	genes	**over/under**	**p-value**	**genes**	**over/under**	**p-value**
p53 signaling pathway	0			4		
Adipocytokine signaling pathway	2			3		
ECM-receptor interaction	1			3		
TGF-beta signaling pathway	1			3		
Cytokine-cytokine receptor interaction	1			2		
Cell adhesion molecules	0			2		
Toll-like receptor signaling pathway	0			2		

List of genes assigned to the over- or under-represented GO terms. Genes in the list are sorted according their cellular function. Significance levels are given as Bonferroni corrected p-values ($p<0.005$) following a chi-square test.